



INFLUENCE OF MATERIAL PROPERTIES ON SHEAR STRENGTH OF URM WALLS RETROFITTED WITH FRP

M.A. ElGawady¹

¹ Dept of Civil and Environmental Engineering, University of Auckland , Private Bag 92019, Auckland , New Zealand, melg003@ec.auckland.ac.nz

ABSTRACT

This paper presents an analytical model for in-plane shear behaviour of unreinforced masonry (URM) walls retrofitted using fibre reinforced polymers (URM-FRP). The proposed model idealizes masonry, epoxy, and FRP in a URM-FRP as different homogenous layers. Then, using principles from the theory of elasticity, the governing differential equation of the system is formulated and solved. A simple computer program was developed to combine the solution of the differential equations with material nonlinearity. The material nonlinearity was represented by step-by-step layer stiffness degradation; after each step the equations are resolved linearly. The proposed basic analytical model allows the fundamental investigation of in-plane shear behaviour of URM-FRP. Effects of epoxy allowable shear stresses and FRP axial rigidity on the shear strength of URM-FRP are examined. In addition, comparisons with three existing models are carried out. Finally, the model shows that there is a threshold with respect to the axial rigidity of the FRP beyond which no increase in shear strength is expected. In other words, adding masonry lateral resistance to the FRP contribution to the shear strength as recommended by existing models is correct up to a certain limit beyond which this addition is not valid.

KEYWORDS: FRP, composites, epoxy, shear analysis, retrofitting, earthquake

INTRODUCTION

FRP provides a promising technique for retrofitting of seismically inadequate URM walls. However, limited design proposals for the shear strength of URM-FRP have been made [1, 2, 3]. In these proposals the following expression is used to evaluate the shear strength (F) of a URM-FRP:

$$F = F_m + F_{FRP} \quad \text{Equation 1}$$

where F_m = shear strength of URM wall; F_{FRP} = contribution of FRP to shear strength of URM-FRP. The main difference between the available proposals lies in the evaluation of F_{FRP} . In the case of FRP applied perpendicularly to the longitudinal member axis on a single-side of a URM wall, the models are briefly discussed. Triantafyllou [1] proposed the following equation for F_{FRP}

$$F_{FRP} = \rho_h E_{FRP} \epsilon_{eff} tL \quad \text{Equation 2}$$

where ρ_h = reinforcement ratio (area fraction) of FRP in the horizontal direction; E_{FRP} = modulus of elasticity of FRP, t = thickness of masonry wall ; L = length of masonry wall ; ϵ_{eff} = effective strain of FRP at failure and can be calculated as follows:

$$\epsilon_{eff} = 0.0119 - 0.0205(\rho_h E_{FRP}) + 0.0104 (\rho_h E_{FRP})^2 \quad 0 \leq \rho_h E_{FRP} \leq 1 \text{ GPa} \quad \text{Equation 3a}$$

$$\epsilon_{eff} = 0.00245 - 0.00065(\rho_h E_{FRP}) \quad \rho_h E_{FRP} > 1 \text{ GPa} \quad \text{Equation 3b}$$

Later on, Triantafillou and Antonopoulos [2] replaced Equation 3 with the following expression:

$$\mathbf{e}_{eff} = \min \left\{ \begin{array}{l} 0.8 \times 0.17 \left(\frac{f_c^{\frac{2}{3}}}{\mathbf{r}_h E_{FRP}} \right)^{0.30} \mathbf{e}_{FRP} \text{ for CFRP and } 0.048 \left(\frac{f_c^{\frac{2}{3}}}{\mathbf{r}_h E_{FRP}} \right)^{0.47} \mathbf{e}_{FRP} \text{ for AFRP (rupture)} \\ 0.8 \times 0.00065 \left(\frac{f_c^{\frac{2}{3}}}{\mathbf{r}_h E_{FRP}} \right)^{0.56} \quad \text{(debonding)} \\ 0.005 \end{array} \right.$$

Equation 4

where f_c = concrete characteristic compressive strength.

AC125 of ICBO [3] uses the following expression for F_{FRP}

$$F_{FRP} = 0.75 \rho_h f_j t L \quad \text{and} \quad f_j = 0.004 E_{FRP} \leq 0.75 f_{FRP,u} \quad \text{Equation 5}$$

where f_j = axial force in FRP; $f_{FRP,u}$ = ultimate tensile strength of FRP. The main drawback of Equations 3 and 4 is that the axial strain in the FRP is estimated based on an empirical function formulated based on tests of reinforced concrete shallow beams. The main drawback of Equation 5 is that a constant value is assumed for axial strain in the FRP regardless of its axial rigidity. This is converse to what is observed during experimental events. Finally, these existing models add the contribution of FRP (F_{FRP}) to the shear strength of the URM wall (F_m) which is assumed as constant; this aspect should be revised since recent investigation [4] shows it is not the case.

NEW SHEAR STRENGTH MODEL FOR URM-FRP

The proposed model idealizes masonry, epoxy, and FRP in a single sided retrofitted URM using FRP as different layers (Figure 1) of isotropic homogenous elastic materials. Then, the governing differential equation of the system is formulated.

The differential element in Figure 2 shows the in-plane shear stresses acting on the masonry (\mathbf{t}_{xy}^m) and FRP (\mathbf{t}_{xy}^f) as well as the two components of the epoxy shear stress ($\mathbf{t}_{zx}^e, \mathbf{t}_{zy}^e$). From Figure 2 and by using equilibrium equations and principles from elasticity [5], the following equation can be written

$$t^f \nabla^2 t_{xy}^f - \frac{G^e}{t^e} \frac{t_{xy}^f}{G^f} + \frac{G^e}{t^e} \frac{t_{xy}^m}{G^m} = 0 \quad \text{Equation 6}$$

where G^e , G^m , and G^f = shear modulus of epoxy, masonry, and fibre, respectively; t^e , t^m , t^f = thickness of epoxy, masonry, and fibre, respectively. In addition, the relation between the external applied shear force/unit length of the wall N_{xy} and the in-plane shear stresses can be written as follows:

$$N_{xy} = t_{xy}^m t^m + t_{xy}^f t^f \quad \text{Equation 7}$$

substituting for τ_{xy}^m from Equation 2 into Equation 1 and dividing by t^f , then

$$\nabla^2 t_{xy}^f - I^2 t_{xy}^f + C_o = 0 \quad \text{Equation 8}$$

$$\text{where } C_o = \frac{N_{xy}}{t^e t^m t^f} \frac{G^e}{G^m}, \lambda^2 = \left(\frac{G^e}{t^e} \right) \left(\frac{1}{t^f G^f} + \frac{1}{t^m G^f} \right)$$

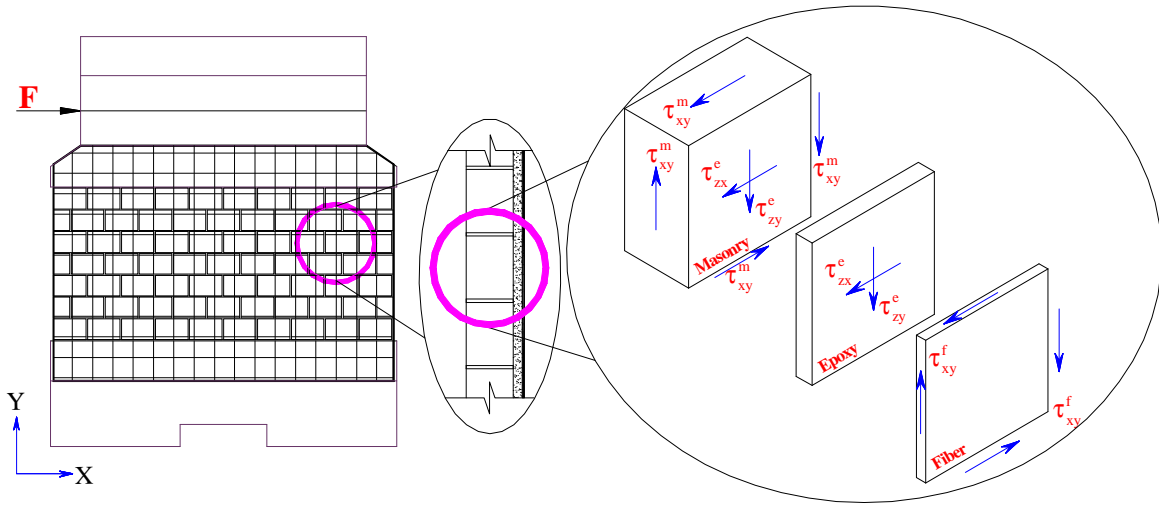


Figure 1 - Single Sided URM-FRP and Differential Element of the Same Retrofitted Wall

The following double Fourier sine series represents a solution [6] of such a differential equation

$$t_{xy}^f = \sum_{m=1}^{\infty} \sum_{n=1}^{\infty} \frac{C_{mn}}{\left(\frac{m\pi}{L} \right)^2 + \left(\frac{n\pi}{h} \right)^2 + I^2} \sin \frac{m\pi x}{L} \sin \frac{n\pi y}{h} \quad \text{Equation 9}$$

$$\text{where } C_{mn} = \frac{4}{Lh} \int_0^a \int_0^b C_o \sin \frac{m\pi x}{L} \sin \frac{n\pi y}{h} dx dy$$

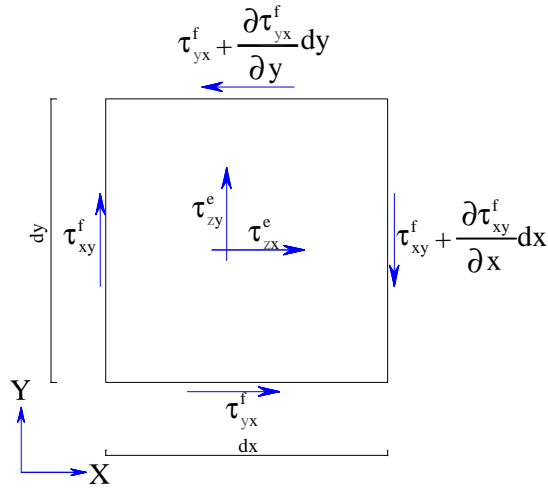


Figure 2 - Shear Stresses Acting on an Element of the Inner Surface FRP Layer

Then, the contribution of the FRP to the shear force can be calculated as follows:

$$F_{FRP} = \mathbf{t}_{xy}^f t^f L \quad \text{Equation 10}$$

The shear force and stresses resisted by the masonry can be calculated as follows:

$$\mathbf{t}_{xy}^m = \frac{F - F_{FRP}}{Lt} \quad \text{Equation 11}$$

Finally, to take into consideration the nonlinearity of the materials, a step-by-step stiffness degradation of masonry as well as epoxy has been implemented in a program (Figure 3) written in MATLAB [7]; note that URM and epoxy layers were assumed to have an elastic perfectly plastic force deformation curves while FRP layer behaves linearly up to failure [5].

PARAMETRIC STUDY

The model was calibrated elsewhere [5]. In this paper the main purpose is to examine: 1) if the effective strain is a constant value (i.e. similar to Equation 5) or variable (i.e. similar to either Equation 3 or 4); 2) the effect of different material parameters (FRP, epoxy, and masonry properties) on the shear strength of URM-FRP, and 3) whether or not F_m is identical for URM and URM-FRP. To achieve these goals, the proposed model was used to examine a given URM wall. The URM wall dimensions are 1565 mm long, 1000 mm height, and 75 mm thick. These dimensions are similar to the dimensions in an experimental work [5].

Three values of epoxy allowable shear stresses were studied: 1.40 MPa (L type), 3.00 MPa (M type), and 6.00 MPa (H type). The effects of applying these epoxy types to different URM walls with different allowable shear stresses are presented in this paper.

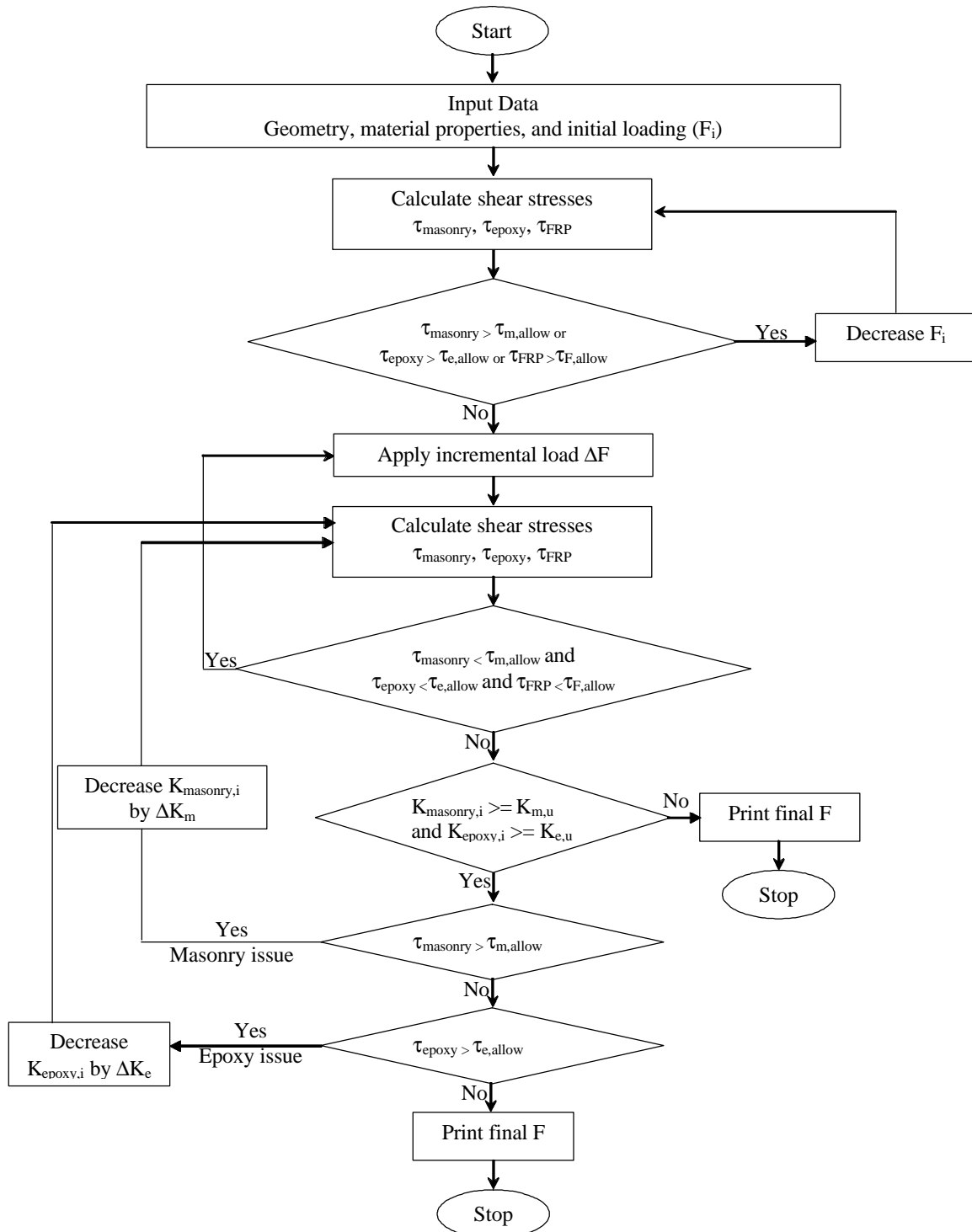


Figure 3 - Flow Chart for Calculating the URM-FRP Lateral Resistance

The URM wall has three different values for allowable shear stresses: 0.25 MPa (L type), 0.50 MPa (M type), 1.50 MPa (H type). An elastic shear modulus of 0.7 GPa was used for the masonry layer. For the epoxy layer, a value of 1.5 GPa was used as an initial shear modulus, based on manufacture data. The results are presented through Figures 4 to 6; in these figures the following abbreviations have been used: Triantafillou [1] = Equation 3; [2] = Equation 4; AC

125 = Equation 5; EIG_M-E = the proposed model where M and E represents masonry and epoxy allowable shear stresses respectively.

Figures 4 and 5 show the comparison between the proposed model and Equation 3. The horizontal axis represents the axial rigidity of the applied FRP (ρE). The vertical axis represents the FRP efficiency (ζ). The FRP efficiency was defined at any axial rigidity (ρE) as follows: the ratio between the stresses in the FRP due to that amount of ρE to the stresses in the FRP due to the lower value of ρE . A lower value of 0.04 GPa was chosen as minimum value for ρE . In general all the curves have trends similar to the one given by Equation 3. Figure 4 shows the comparisons in the case of masonry of Type M. The figure shows that the rate of degradation of ζ is very high for epoxy Types M and L. This is due to the fact that for epoxy Type L the limit on epoxy stiffness degradation dominates the URM-FRP behaviour for all amounts of ρE . Similar explanation can be given for case of M epoxy type. In case of H epoxy type (Figure 4), the limit on masonry stiffness degradation dominates the URM-FRP shear behaviour until approximately ρE equal to 0.14 GPa. For ρE less than or equal to 0.14 GPa, the rate of degradation of ζ is very slow. For ρE greater than 0.14 GPa, the limit on epoxy stiffness degradation dominates the URM-FRP shear behaviour with a higher degradation rate of ζ . Note that, the degradation rate given by Equation 3 appears to be an average of the different degradation rates given by all types of epoxy.

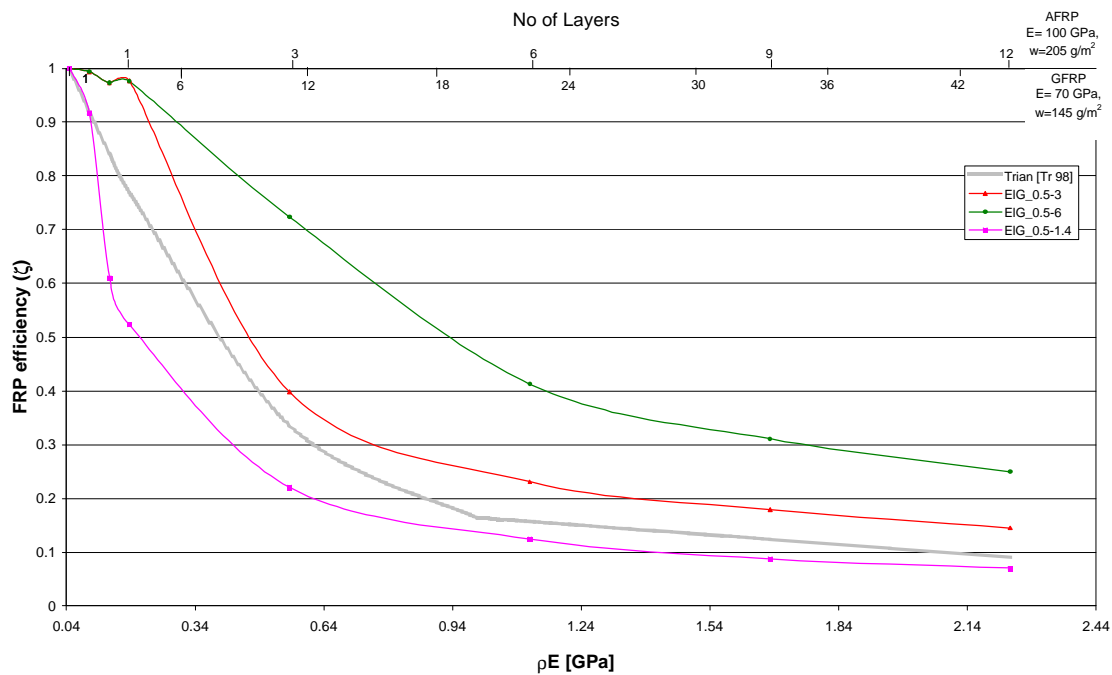


Figure 4 - Effect of Using Type M Masonry (0.50 MPa) with Epoxy Having Different Allowable Shear Stresses on FRP Efficiency (ζ)

For masonry Type L (Figure 5), the degradation rate given by Equation 3 seems as a lower bound for all types of epoxy. Based on this note, one can say that the degradation rate given by Equation 3 is close to an average of all the degradation rates given by different epoxy and masonry parameters. This is expected since Equation 3 was empirically developed.

Figures 4 and 5 show that the axial rigidity of the FRP is not the only factor that influences the effective strain in FRP. For all masonry types (L, M), the epoxy type influences the rate of degradation of ζ : the higher the allowable shear stress of epoxy, the lower the rate of degradation of ζ . It appears that when masonry dominates the behaviour of URM-FRP there is less “losses” in FRP effective strain. Finally, careful examination of the figures shows that there are three phases for ζ degradation rate. The first phase when ρE less than or equal to approximately 0.19 GPa, if epoxy dominates the behaviour ζ degradation rate is very high. The second phase when ρE between 0.19 and 1.12 GPa, ζ degradation rate is slower than the previous phase. The third phase when ρE is greater than or equal to 1.12 GPa, ζ degradation rate is very slow and regardless of the material parameters (except masonry Type L – epoxy Type H) all the efficiency curves are approximately parallel to the curve that comes from Equation 3b. Note that, Equation 3 used value of $\rho E = 1$ GPa as the limits between two phases of the degradation rate curve.

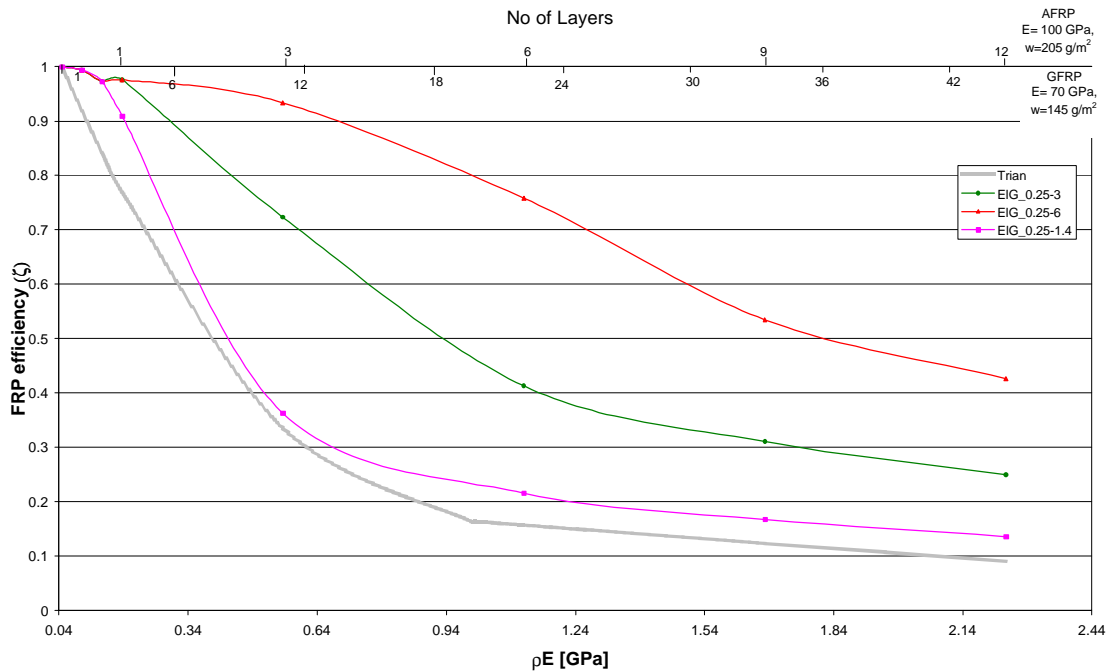


Figure 5 - Effect of Using L Type Masonry (0.25 MPa) with Epoxy Having Different Allowable Shear Stresses on FRP Efficiency (ζ)

Regarding shear strength of URM-FRP, comparisons between the proposed model and the existing models are presented (Figure 6) for the three types of epoxy and only for masonry Type M due to space limitations in this paper. In general, all the curves tend to be a mix of Equations 3 and 4. However, the absolute values of F are close to the values predicted by Equation 4. Equation 4 seems to be an average of the different F estimated using different material properties. The divergence between the estimated F according to the proposed model and Equation 4 is influenced by material properties. In addition, Equation 3 estimated F higher than the proposed analytical model. The high difference between Equation 3 and the proposed model is expected since Equation 3 implicitly assumes wrapped retrofitting. Recall that in case of wrapped retrofitting, FRP rupture is the most probable mode of failure. Finally, by increasing

epoxy allowable shear stress the lateral resistance of URM-FRP increases. Regarding Equation 5, this equation underestimated F for small values of FRP axial rigidity and overestimated F for high values of FRP axial rigidity. However, until ρE of 0.19 GPa, Equation 5 estimated F too close to the average of F estimated using masonry type M and different epoxy types.

Also, Figure 6 shows that by increasing epoxy allowable shear stress F increases. However, the increment in F is approximately linear till a certain amount of ρE let's say $(\rho E)_{\text{optimum}}$. Increasing ρE beyond $(\rho E)_{\text{optimum}}$ has a less significant effect on F. This $(\rho E)_{\text{optimum}}$ can be used as cost effective limits as suggested by other researchers [4 and 1]. However, $(\rho E)_{\text{optimum}}$ is not a constant value. It changes with changing material properties. For the same masonry type, by improving epoxy type, $(\rho E)_{\text{optimum}}$ increases with high increment in corresponding F.

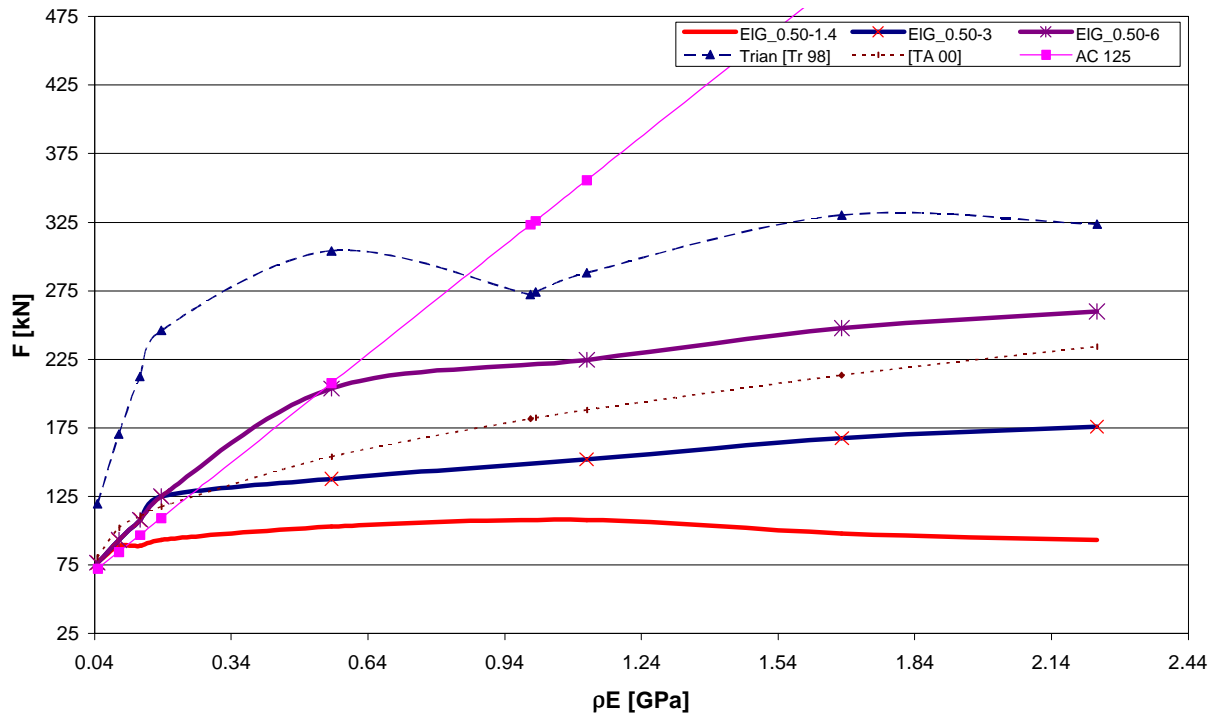


Figure 6 - Effect of using M masonry (0.50 MPa) with epoxy having different allowable shear stresses on URM-FRP lateral resistance

Figure 7 shows the gain in the lateral resistance in terms of ρE for the different epoxy and masonry types. The gain is defined as follows:

$$\text{Gain} = \frac{F - F_m}{F_m} \% \quad \text{Equation 12}$$

Figure 7 shows that by increasing epoxy allowable shear stress the gain in the shear strength increases. In contrast, by increasing masonry allowable shear stress the gain in the shear strength reduces. A similar phenomenon is observed for RC beams [4]. Finally, for the same epoxy and masonry allowable shear stress, by increasing ρE , the gain increases until a certain upper limit $(\rho E)_{\text{limit}}$; beyond this limits any increment in ρE leads to reduction in the gain. The $(\rho E)_{\text{limit}}$ is

influence by epoxy and masonry properties. This reduction in F is due to the following: beyond $(\rho E)_{\text{limit}}$ URM-FRP reaches the limit on epoxy stiffness degradation before the masonry reaches its allowable shear stress. However, after failure of FRP the lateral resistance of URM-FRP reduced to the lateral resistance corresponding to URM wall. In this context the amount of gain depends on the definition of failure: if failure is defined at failure of FRP then it is possible to have negative gain; since at failure of FRP, the masonry wall does not develop its ultimate lateral resistance. If failure defined at certain reduction in lateral resistance (e.g. 20-30% of the lateral resistance), then after rupture of FRP the URM wall alone will continue to develop its lateral resistance until it reaches its ultimate lateral resistance.

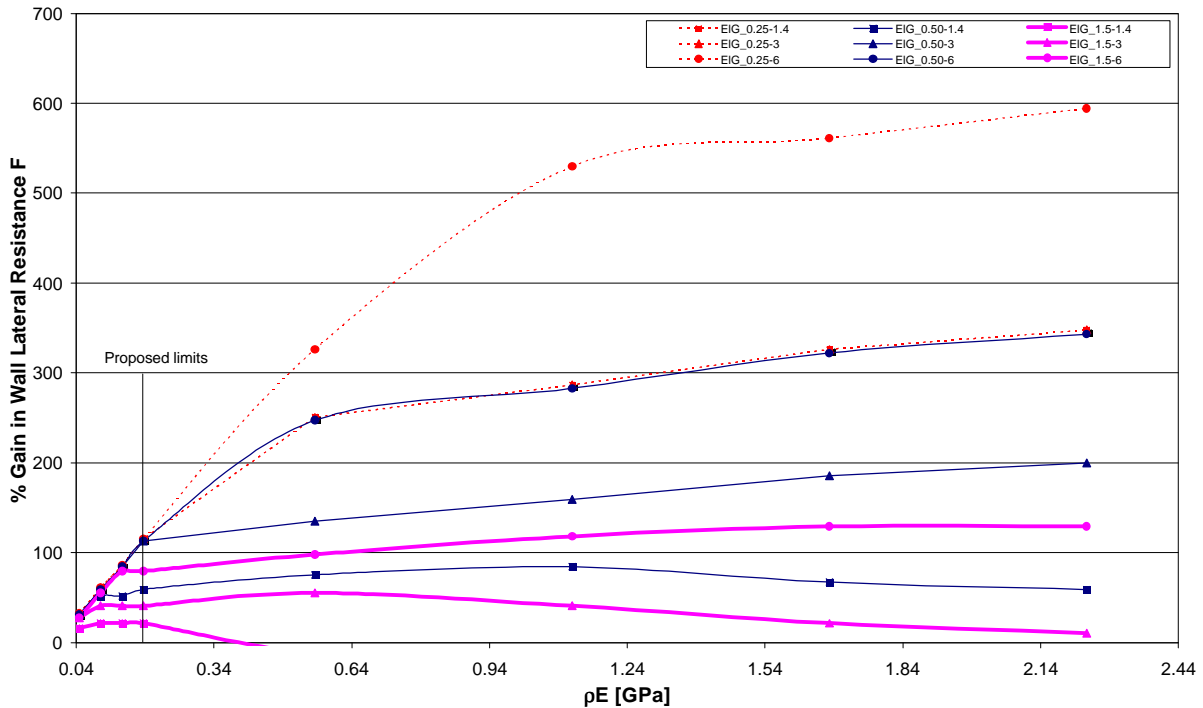


Figure 7 - Effect of using different masonry with epoxy having different allowable shear stresses on gain in wall lateral resistance

The previous remark leads to an important conclusion: using Equation 1 (i.e. adding masonry lateral resistance to FRP contribution) is correct until a certain limit beyond this limit this equation is no longer valid. To avoid such invalidity in the equation and in order to have cost effective use of FRP it is proposed that $(\rho E)_{\text{limit}}$ be limited to a value of 0.19 GPa. For material properties examined here, this value is smaller than $(\rho E)_{\text{limit}}$ and $(\rho E)_{\text{optimum}}$ which mean safe economic design. For RC beams [4], it was observed that beyond a value of 0.005 for $\rho E/f_c^{0.67}$ F tends to stabilized and they proposed to use such value as a criterion for cost effective design. If typical values of existing masonry compressive strength are considered (4-7 MPa) with this proposed limit, then the cost effective design criterion is corresponding to ρE of 0.13-0.17 GPa which corresponds well to the proposed value estimated by the analytical model. In light of Figure 7, the proposed limit on ρE is appropriate for all material properties except for H epoxy. In the later case, a value of 0.54 GPa is more appropriate.

CONCLUSIONS

The results show that the axial strains in FRP are inversely proportional to the FRP axial rigidity. However, it is not possible to have a single function to represent the relation between ρE and FRP axial strain. The relation between the two quantities depends on several factors (e.g. allowable shear stresses in epoxy and masonry). For high values of ρE (above approximately 1.12 GPa), it is possible to use a single function to describe that relationship.

The higher the allowable shear stresses in epoxy are, the higher F ; the increment in epoxy allowable shear stresses could be achieved by the development of new materials or by using mechanical anchorage systems at the boundaries. As expected, the effect of such mechanical anchorage systems is higher for high values of ρE .

The proposed model quantifies the relation between F_m and F_{FRP} . The results show that adding F_{FRP} to F_m is only valid to certain limit. Beyond this limit, any additional increment in the axial rigidity of FRP has no effect. In other words, there is a threshold with respect to the axial rigidity of the FRP beyond which no increase in shear gain is expected. Such a threshold can be used as a criterion for a cost effective design. Such limit on ρE depends on the material allowable stresses and ductility. A value of 0.19 GPa can be proposed as a limit on ρE , which covers the practical values of material properties.

This research shows that much information is needed to refine characterizations of the materials used in URM-FRP system (i.e. masonry, epoxy, FRP). The proposed model, which describes how URM-FRP behaves due to in-plane loading, can contribute to classify the needed development.

ACKNOWLEDGMENTS

The work presented here was originally part of the author's PhD. at the Swiss Federal Institute of Technology at Lausanne (EPFL). The author thanks Professor M. Badoux and Dr. P. Lestuzzi for their valuable suggestions during the thesis preparation.

REFERENCES:

1. Triantafillou, T. Strengthening of masonry structures using epoxy-bonded FRP laminates. *J. Comp. for Constr., ASCE*, 2(2), 1998, P. 96-104.
2. Triantafillou, T. Antonopoulos, C. Design of concrete flexural members strengthened in shear with FRP. *J. Comp. for Constr., ASCE*, 4(4), 2000, P. 198-205.
3. ICBO, AC125. Acceptance criteria for concrete and reinforced and unreinforced masonry strengthened using fiber-reinforced polymers (FRP), composite systems, 2001.
4. Bousselham, A., Chaallal, O. Shear strengthening RC beams with FRP: assessment of influencing parameters and required research. *ACI Struct. J.* 101(2), 2004, P. 219-227.
5. ElGawady, M, Seismic in-plane behavior of URM walls upgraded with composites. PhD. Thesis, IS-IMAC-ENAC, Swiss Federal Institute of Technology. 2004.
6. Kim, H., Kedward, K. Stress analysis of in-plane shear loaded adhesively bonded composite joints and assemblies," Office of aviation research, Report No. DOT/FAA/AR-017, 2001.
7. MATLAB Version 6.5.1 The language of technical computing, the Mathworks Inc. 2002